

Substrate Diversity of Herpes Simplex Virus Thymidine Kinase

IMPACT OF THE KINEMATICS OF THE ENZYME*

(Received for publication, May 18, 1999, and in revised form, August 4, 1999)

Beatrice D. Pilger‡, Remo Perozzo‡, Frank Alber§¶, Christine Wurth‡, Gerd Folkers‡,
and Leonardo Scapozza‡¶

From the ‡Department of Pharmacy, Swiss Federal Institute of Technology, Winterthurerstrasse 190,
CH-8057 Zürich, Switzerland and the §Istituto Nazionale per la Fisica della Materia and
¶International School for Advanced Studies, Via Beirut 4, 34014 Trieste, Italy

Herpes simplex virus type 1 (HSV 1) thymidine kinase (TK) exhibits an extensive substrate diversity for nucleobases and sugar moieties, in contrast to other TKs. This substrate diversity is the crucial molecular basis of selective antiviral and suicide gene therapy. The mechanisms of substrate binding of HSV 1 TK were studied by means of site-directed mutagenesis combined with isothermal calorimetric measurements and guided by theoretical calculations and sequence comparison. The results show the link between the exceptionally broad substrate diversity of HSV 1 TK and the presence of structural features such as the residue triad His-58/Met-128/Tyr-172. The mutation of Met-128 into a Phe and the double mutant M128F/Y172F result in mutants that have lost their activity. However, by exchanging His to form the triple mutant H58L/M128F/Y172F, the enzyme regains activity. Strikingly, this triple mutant becomes resistant toward acyclovir. Furthermore, we give evidence for the importance of Glu-225 of the flexible LID region for the catalytic reaction. The data presented give new insights to understand mechanisms ruling substrate diversity and thus are crucial for both the development of new antiviral drugs and engineering of mutant TKs apt to accept novel substrate analogs for gene therapeutic approaches.

Herpes simplex virus type 1 (HSV 1)¹ thymidine kinase (TK) is a multifunctional enzyme that possesses kinase activities normally performed by three separate cellular enzymes. It phosphorylates thymidine (dT), which is then transformed by cellular kinases to the triphosphorylated DNA building block, and deoxyuridine (dU); both reactions are comparable to the function of human cellular TK. Further, it converts deoxycytidine (dC) to dCMP, as does human deoxycytidine kinase (dCK), and phosphorylates thymidylate (dTMP), as does human TMP kinase (TmpK) (1–3). Moreover, unlike its cellular counterpart human cellular TK, HSV 1 TK is able to phosphorylate pyrimidine, as well as purine analogs, and discloses low stereochemical demands for the ribose moiety, as it also accepts acyclic side chains as phosphoryl group acceptors *e.g.* (4–6). These

differences in substrate diversity are the crucial molecular basis for the selective treatment of viral infections. Nowadays, the most widely used therapeutic compounds to interfere with a severe HSV 1 infection are the purine analogs acyclovir (ACV) and penciclovir and their prodrugs valaciclovir and famciclovir, respectively. They require HSV 1 TK to be efficiently activated in order to block virus proliferation by inhibition of viral DNA polymerase. HSV 1 TK is the key enzyme in this antiviral strategy. In gene therapy of cancer (7, 8) and AIDS (9), HSV 1 TK is used as a suicide enzyme in combination with the purine analog ganciclovir. Another important application is the use of HSV 1 TK as a rescue system in allogeneic bone marrow transplantation-induced graft *versus* host disease (10). In addition to the significance from a therapeutic point of view, HSV 1 TK seems to be important for the reactivation of the virus from lifelong latent infection in neuronal ganglia (11–13). However, there is evidence that human TK can functionally replace viral TK in terms of reactivation of the virus from latency (14).

There are no recognizable sequence similarities between HSV 1 TK and human cellular TK (15). Rather, sequence alignments have detected similarities between herpesvirus TKs and human dCK (16) and to a lesser extent cellular TmpK (17). Despite the limited sequence homology with enzymes of the nucleotide kinase (NK) family, HSV 1 TK shares structural features comprising a parallel five-stranded β -sheet and a glycine-rich loop common to all NKs. In the crystal structure, HSV 1 TK is a homodimeric enzyme with 376 amino acids per subunit (18–20). The two subunits are related by C2 symmetry. The active site is formed by an ATP- and a nucleoside-binding region. The visual representation of the thymidine binding site is depicted in Fig. 1, featuring a complex hydrogen bond network within the active site. The thymine ring makes pairwise hydrogen bond interaction via its 4-carbonyl and 3-NH group with the amide group of the highly conserved Gln-125 and hydrogen bonds with Arg-176 by means of two ordered water molecules. Moreover, the pyrimidine ring of thymidine is fixed between Met-128 and Tyr-172, forming a sandwich-like complex. His-58 and Arg-163 both interact with the hydroxyl group of Tyr-172, sealing the position of tyrosine. The deoxyribose makes hydrogen bond interaction via its 3'-OH with Tyr-101 and the highly conserved Glu-225 and via its 5'-OH with Glu-83. Glu-225 belongs to the LID domain, a region rich in lysine and arginine residues that appears to be able to form a flap that encloses the active site. This LID region is expected to undergo conformational changes upon substrate binding and therefore influencing the catalytic phosphorylation rate, similar to ADK, with which TK shares similar three-dimensional features (21).

Up to now, various studies (see, *e.g.* Refs. 22–25) tried to

* The costs of publication of this article were defrayed in part by the payment of page charges. This article must therefore be hereby marked "advertisement" in accordance with 18 U.S.C. Section 1734 solely to indicate this fact.

¶ To whom correspondence should be addressed. Tel.: 41-1-635-6071; Fax: 41-1-635-6884; E-mail: scapozza@pharma.ethz.ch.

¹ The abbreviations used are: HSV 1, herpes simplex virus type 1; TK, thymidine kinase; dT, thymidine; dC, deoxycytidine; dCK, deoxycytidine kinase; dTMP, thymidine monophosphate; TmpK, thymidylate kinase; ACV, acyclovir; PCR, polymerase chain reaction; DTT, DL-dithiothreitol; HPLC, high performance liquid chromatography; AZT, 3'-azidodeoxythymidine; ITC, isothermal titration microcalorimetry.

elucidate the role and functionality of the amino acid residues in HSV 1 TK, and with resolving of the crystal structure (18–20), pivotal supplementary information became accessible. For example, this structural information allowed researchers to render comprehensible (29) some of the mechanisms responsible for development of herpesviral resistance, an increasing problem in clinics in the treatment of immunocompromised patients (26–28). Despite the increased structural knowledge, the basis of the molecular difference in substrate and drug specificity of HSV 1 TK and the particular role of the LID region still remain unclear. This work reports a study on the nature of mechanism of binding of HSV 1 TK by means of site-directed mutagenesis combined with isothermal calorimetric measurements and guided by *ab initio* calculations and sequence comparison. It shows the link between the broad substrate diversity of HSV 1 TK and the presence of structural features, such as the residue triad His-58/Met-128/Tyr-172, which is thought to confer distinctive binding of an exceptionally large variety of substrates to the HSV 1 TK and to guide the catalytic properties. Furthermore, we give evidence for the importance of the flexible LID domain for enzyme function.

EXPERIMENTAL PROCEDURES

Materials—[methyl-1',2'-³H]Thymidine (3 TBq/mmol) was obtained from Amersham Pharmacia Biotech, and [side chain-2-³H]acyclovir (1.2 TBq/mmol) was obtained from NEN Life Science Products. 3'-Azido-[methyl-³H]deoxythymidine (0.2 TBq/mmol) was purchased from Moravsek Biochemicals. Nucleotides and AmpliTaq Gold™ polymerase were bought from Perkin-Elmer. Restriction endonucleases, T4 DNA ligase, and thrombin were from Promega. Reagents for enzyme assays were obtained from Sigma.

Strains and Plasmid—Strain DH5 α (*deo^R endA1 recA1 rel A1 gyrA96 thi-1 hsdR17 supE44 lacZ Δ M15 F⁻ λ ⁻*) (CLONTECH) was used for all cloning steps. Strain BL21 (*ompT⁻, F⁻, hsdS (rB⁻, mB⁻), gal*) (Amersham Pharmacia Biotech) served as host for expression. The plasmid pGEX-2T was purchased from Amersham Pharmacia Biotech. The plasmid pBR322-TK containing the gene for HSV 1 strain F TK was a gift from S. McKnight. The expression vector pGEX-2T-TK was constructed as described earlier (30).

Mutagenesis—Site-directed mutagenesis was performed by using oligonucleotide-directed polymerase chain reaction based on a three-primer method (31, 32). The primers were ordered, synthesized, and purified at Microsynth (Balgach, CH). Briefly, in the first PCR, bacteriophage M13mp18, containing the *Bam*HI-*Kpn*I fragment of HSV 1 TK, was amplified using the respective antiparallel mutagenic primer (H58L, 5'-GAC GGT CCC CTC GGG ATG GG-3'; M128I, 5'-CAG ATA ACA ATC GGC ATG CC-3'; M128A, 5'-GCG CCC AGA TAA CAG CCG GCA TGC CTT ATG C-3'; M128F, 5'-GCG CCC AGA TAA CAT TCG GCA TGC CTT ATG C-3'; Y172F, 5'-CTC CTG TGC TTC CCG GCC G-3') and the M13mp universal primer (5'-GCT ATG ACC ATG TTA CG-3'). The resulting amplification products were gel-purified and subsequently used as a megaprimer. In the second PCR, the isolated megaprimer was hybridized to pGEX-2T-TK and extended within a single PCR cycle. Then, the flanking M13mp universal primer and pGEX-2T universal primer (5'-GGG CTG GCA AGC CAC GTT TGG TG-3') were added to the PCR tubes, and 30 PCR cycles were performed. In the last step, each of the fragments containing the desired mutation was cloned into the expression vector pGEX-2T-TK by digestion with the restriction enzymes *Bam*HI and *Kpn*I and subsequent gel purification and ligation. Additional restriction steps with *Bam*HI/*Sac*I and *Bam*HI/*Acc*I, were necessary to obtain the mutants M128F/Y172F, H58L/M128F/Y172F, and H58L/M128F.

For the mutant E225L, we used a four-primer-based PCR method described by Innis *et al.* (33). Basically, two primary PCRs are performed separately. The mutation is introduced as part of the respective mutagenic inside primers (forward, 5'-CCC GGG CCT GCG GCT GGA CC-3'; reverse, 5'-GGT CCA GCC GCA GGC CGG G-3'), each of which is amplified with a suitable outside primer. The two products overlap in sequence; both contain the same mutation. After gel purification, these overlapping primary products were denatured and allowed to reanneal together, producing two possible heteroduplex products. The subsequent reamplification of one of these products with only the right- and leftmost ("outside") primers resulted in the enrichment of the full-length, secondary product, which was then introduced into the vector

pGEX-2T-TK, replacing the respective wild type fragment by *Sma*I/*Sac*I restriction.

Sequence Verification—Competent *Escherichia coli* DH5 α was transfected with the mutated pGEX-2T-TK DNA. After DNA isolation of several clones, we sequenced the entire TK gene of the respective mutant progeny, using the dye terminator method (ABI PRISM™ 310) to verify that the targeted mutation and no frameshift or additional mutation had occurred.

Expression and Purification of the Mutant HSV 1 TKs—Competent *E. coli* BL21 were transformed with the vector pGEX-2T-TK containing the respective mutated full-length *tk* gene as a glutathione *S*-transferase fusion protein. Protein expression was induced by the addition of 0.2 mM isopropyl- β -D-thiogalactopyranoside. After 20 h at 25 °C, bacteria were harvested by centrifugation, frozen, thawed, and lysed in buffer (50 mM Tris, pH 7.5, 1 mM phenylmethylsulfonyl fluoride, 10 mM DTT, 10% glycerol, and 1% Triton X-100) in the presence of 150 μ g/ml lysozyme and 2000 units of DNase I (10 mM MgCl₂, 1 mM MnCl₂, and 10 mM EDTA for inactivation of DNase I afterward) for 30 min at 4 °C and by additional sonication for 3 min. The lysate was clarified by centrifugation at 12,000 $\times g$ for 20 min and subjected to a one-step glutathione-agarose purification procedure and subsequently to column thrombin cleavage as described (34). Purification was monitored by SDS-polyacrylamide gel electrophoresis and led to a >90% pure thrombin-cleaved protein, which was directly used for kinetic studies. Total protein concentration was measured using the Bio-Rad protein assay.

Thymidine, Acyclovir, and AZT Kinetics—Kinetic studies measuring the conversion of the labeled substrate to substrate monophosphate were performed using the DEAE-cellulose method as described earlier (35, 36). Reactions were carried out in a final volume of 30 μ l containing 50 mM Tris, pH 7.2, 5 mM ATP, 5 mM MgCl₂, 1.5 mg/ml BSA. The amount of enzyme and concentrations of ³H-labeled substrate were chosen in consideration of Michaelis-Menten conditions for initial velocity measurements. The K_m and V_{max} values have been determined by nonlinear fit of the raw data to the Michaelis-Menten equation using the Microcal Origin software. k_{cat} values were determined by dividing V_{max} by the enzyme concentration. These values were measured based on at least three independent assays.

Spectrophotometric Assay for Thymidine Kinase Activity—A UV-spectrophotometric test was employed to monitor ADP formation during substrate phosphorylation. Enzyme activity was measured using a lactate dehydrogenase-pyruvate kinase-coupled assay (6). The change in A_{340} was recorded over time by analyzing mutant TKs and different substrates.

HPLC Assay—High performance liquid chromatography was applied to monitor ADP and dTMP, ACVMP, or AZTMP formation during substrate phosphorylation with ion-pair chromatography using a modified version of the previously published protocol (37) (Column, RP-18; solvent, 0.2 M NaH₂PO₄, 25 mM tetrabutylammonium-hydrogen sulfate, 3% methanol; flow, 1.1 ml/min; detection, UV 254 nm). This method was applied to check those mutants that could not be measured by either the radioactive or the UV spectrometric approach. Reactions were carried out in a final volume of 75 μ l containing 50 mM Tris, pH 7.2, 5 mM ATP, 5 mM MgCl₂, 2 mM thymidine (ACV/AZT), and 1–5 μ g of thymidine kinase. The reaction was stopped after 1 h at 37 °C by a 10-fold dilution in water and freezing at -20 °C prior to injection. The formation of the nucleotide monophosphate was monitored qualitatively. Two different blank reactions (no enzyme or no substrate) were run concurrently to account for the occurring minimal reaction independent ATP hydrolysis. The detection limit for phosphorylated substrate lies under 20 nM making this method even more sensitive than the UV assay.

Titration Calorimetry—To evaluate the binding affinity of the less active mutants, isothermal titration microcalorimetry (ITC) was carried out. For stability reasons, all measurements were performed with the glutathione *S*-transferase fusion protein because the biochemical properties are identical to thymidine kinase (34). After isolation of the fusion protein from the crude extract onto the glutathione-Sepharose, the protein was directly (on-column) exchanged into the measuring buffer (50 mM Tris-HCl, pH 7.5, 4 mM EDTA, 5 mM glutathione, 1 mM DTT, and 1 mM ATP) by thoroughly rinsing the column with an excess amount of buffer. The purified protein was eluted by addition of 5 mM glutathione into the buffer and was directly used for titration experiments. The enzyme concentration was determined using the Bio-Rad protein assay and was corrected for impurities detected by SDS-polyacrylamide gel electrophoresis and quantified by gel densitometry. This purification protocol usually let to a purity of 70–80% of the fusion protein.

Isothermal titration microcalorimetry was performed employing an OMEGA microcalorimeter from Microcal, Inc. (Northampton, MA), with

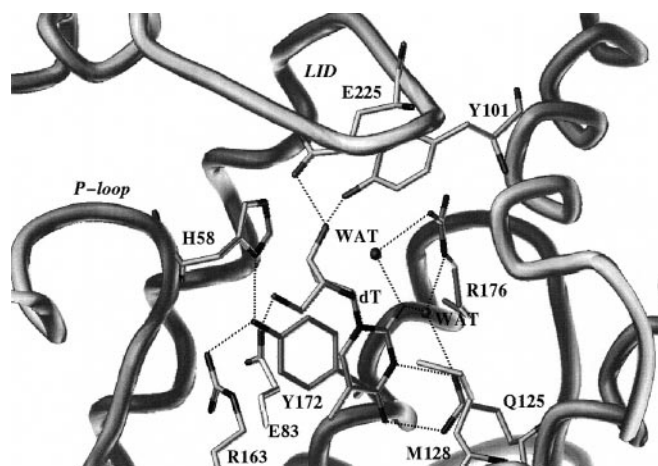


FIG. 1. Representation of a portion of the active site of HSV 1 TK with bound thymidine. The position and geometry of dT and the amino acids that are directly involved in substrate binding are shown as capped sticks and are labeled (18). The secondary structure of the protein is displayed as tubes. The hydrogen bond-mediating water molecules are presented as small spheres, and hydrogen bonds are displayed as dashed lines. The LID region and P-loop (glycine loop) are indicated. The figure was prepared using the program SYBYL, version 6.3 (Tripos Associates). The coordinates are indexed as 2VTK in the Protein Data Bank, Rutgers University.

a cell volume of 1.3338 ml and using a 100- μ l microsyringe while stirring at 375 rpm. The calorimeter and the equations used to fit calorimetric data have been described in detail previously (38). The reference cell was filled with water containing 0.01% sodium azide, and the instrument was calibrated with standard electrical pulses. All ITC measurements were performed at 25 $^{\circ}$ C in 50 mM Tris-HCl, pH 7.5 (at 25 $^{\circ}$ C), 4 mM EDTA, 5 mM glutathione, 1 mM DTT, and 1 mM ATP. Prior to loading into the microcalorimeter, all solutions were degassed for 10 min with gentle swirling under vacuum. Solutions of the fusion protein were filled in the sample cell and titrated with thymidine with a first control injection of 1 μ l followed by 29 identical injections of 4 μ l. Thymidine solutions were prepared by dissolving it in the same buffer to concentrations generally 25 times higher than the protein solution. The titration experiment was designed to ensure complete saturation of the enzyme before the final injection. The heat of dilution for the ligand was concentration-independent and corresponded very well to the heat observed from the last injections after the protein was saturated. Therefore, the baseline of the titrations could usually be well estimated from the last injections of the titration. No interference of spontaneous DTT oxidation with measurements was observed. Data were collected, corrected for ligand heats of dilution, and deconvoluted using the Microcal Origin software supplied with the instrument to yield binding constants (K_m) and enthalpies of binding (ΔH). The thermodynamic parameters were calculated from the basic equations of thermodynamics: $\Delta G = \Delta H - T\Delta S = -RT\ln K_m$, where ΔG , ΔH , and ΔS are the changes in free energy, enthalpy, and entropy of binding, respectively.

Sequence Alignments—Sequences were taken from the GenBankTM data base and were aligned with the aid of the program multAlin (39).

RESULTS

Sequence Alignments—Two sequence motifs (GXXGXGK and (F)DRH) are highly conserved among thymidine kinases. The region GXXGXGK corresponds to the glycine-rich loop (22), which accommodates the ATP-phosphate, and the (F)DRH motif (40) is located in the five-stranded β -sheet core of the protein (18–20). Based on the sequence alignment shown in Fig. 2, we analyzed the residues that are involved in thymidine fixation and in deoxyribose orientation (Glu-225) (see Fig. 1). Gln-125, Arg-163, and Glu-225 are highly conserved in all TKs. The succession of His-58, Met-128, and Tyr-172 in TKs is so far known for four viral strains, namely HSV 1, HSV 2, MHV (Fig. 2), and BHV. Instead, in most other TKs the combination X-58/Phe-128/Phe-172 is found, where X can be any hydrophobic amino acid except histidine. In all the studied TKs, a Tyr at

position 172 is never combined with a Phe at position 128 (HSV 1 TK numbering).

Substrate Diversity and Induced Fit—To address mechanisms guiding substrate specificity and the role of amino acids in substrate fixation within the active site of HSV 1 TK, we studied eight different mutants of HSV 1 TK. Moreover, the role of the negatively charged Glu-225 sitting within the supposedly moving, otherwise positively charged LID region, was studied by means of an additional mutant. The purification and expression scheme allowed rapid isolation of milligram amounts of wild type and mutant HSV 1 TK enzyme. The two additional unspecific cleavage sites for thrombin within TK led to a truncated TK, lacking the N-terminal 33 amino acids that are not essential for catalytic activity (41).

Previously performed *ab initio* calculations, using the Carr-Parrinello approach, clearly indicated that the molecular orbitals of Met-128 and Tyr-172 do not overlap with those of the substrate, nor are π - π interactions between the Tyr-172 ring and the substrate present (42). Interestingly, no polarization effect was found on the Met sulfur atom. This indicated that sulfur has only a hydrophobic effect, although it is a highly polarizable element. Instead, strong polarization effects were located on the substrate, especially on the O and N atoms. Electrostatic interactions between tyrosine and thymine can therefore play an important role in substrate fixation. In order to verify the results and predictions of the *ab initio* calculations and the alignments, site-directed mutagenesis at positions 58, 128, and 172 has been performed. The results of these experiments are summarized in Table I.

M128A—The replacement of methionine at position 128 by an alanine led to a loss of enzyme activity, pointing out the important role of a rather bulky residue at position 128 for substrate fixation.

M128I—Interestingly, the exchange of methionine by isoleucine resulted in the same activity as the wild type enzyme.

M128F—With phenylalanine at position 128, a completely inactive enzyme emerged. Even with the HPLC system, no phosphorylated product was observed.

Y172F—Exchange of tyrosine 172 to phenylalanine, which entails the loss of hydrogen bonds to His-58 and Arg-163 (see Fig. 1), led to an enzyme with an altered activity profile. Under standard kinetic conditions, no explicit progressive thymidine phosphorylation was detectable, but by increasing the pH of the reaction mixture, the kinetics were measurable, indicating a different pH sensitivity profile of this mutant in comparison with the wild type enzyme. However, under the adapted conditions, the K_m of the mutant toward thymidine remained within the same order of magnitude compared with the wild type.

H58L—To elucidate the role of His within the context of the stringent triad His/Met/Tyr, we established the single mutant H58L. Surprisingly, the K_m for thymidine was largely increased (\sim 600-fold), and the reduction in k_{cat} was about 60-fold. With the UV and HPLC assays, the phosphorylation of neither deoxycytidine nor acyclovir was detectable.

M128F/Y172F—Combination of the inactive mutant M128F with Y172F, creating the “double-F sandwich” enclosing thymidine, did not show any activity, nor was any phosphorylation detected with the HPLC assay. To ensure that no hydrophobic collapse was initiated by the mutations, CD spectra were recorded. However, comparison of mutant CD spectra with the wild type spectrum² revealed no discrepancy. This particular Phe/Phe-combination is encountered in TKs (Fig. 2) but with the difference that no His is found at position 58 (HSV 1 TK numbering).

² B. D. Pilger, unpublished observation.

FIG. 2. Multiple alignment of amino acid sequences of HSV 1 and related virus strains thymidine kinases. Residues of interest are marked using numbering of HSV 1 TK. Selected excerpts of TKs from herpes simplex virus types 1 and 2, marmoset herpesvirus (MHV), equine herpesvirus type 4 (EHV), varicella-zoster virus (VZV), and Epstein-Barr virus (EBV) are displayed. Asterisks denote positions that appear to be completely conserved in all herpesviral TK sequences. Sequences were taken from the GenBank™ data base.

	58 **																					
HSV1	GPHG	MGKTTT	T	QLLVALGS	RDDI	VYVPE	PMTYWRV	VLGA	SETIANIYTT	QHRLDQGEIS												
HSV2	GPHG	VGKTTT	SAQL	MEALGP	RDNI	VYVPE	PMTYWQV	VLGA	SETLNTIYNT	QHRLDRGEIS												
MHV	GPHG	VGKSTT	AEAL	VARCEP	RRPIR	SMLQE	PMAYWRST	FA	SDAITFEYDT	QHRLDSNEIT												
EHV	GVY	GIGKSTT	GRV	MASAASG	GSPT	LYFPE	PMAYWR	TLFE	TDVISGIYDT	QNRKQGGNLA												
VZV	GAV	GIGKTTA	AEEF	LHFHAI	TPNR	ILLIGE	PLSYWR	NLAG	EDAITCGIYGT	QTRRLNGDVS												
EBV	GAP	VGKTTM	LNHL	KAVFG	..	DLTIVVPE	PMRYWTHVY		ENAIKAMHKN	VTRARHGR..												
			* 128						***													
HSV1	AGDA	AVVM	TS	AQIT	MG	MPYA	VTD	AVL	LAPHI	GGEAGSSHAP	PPA....LT	LIFDRHPIAA										
HSV2	AGEA	AVVM	TS	AQIT	MG	STPYA	ATD	AVL	LAPHI	GGEAVGPQAP	PPA....LT	LVFDRHPIAS										
MHV	AAEA	GAFM	TS	LQLH	MG	TPYA	LLE	EAM	RPHV	GRELAEPDDN	GPLPQR	DFV	LVVDRHAVAS									
EHV	VDDA	ALIT	TAH	YQSR	FT	TPYL	ILH	DHT	CTLF	GGNSLQ	RGTQ	P.....DLT	LVFDRHPVAS									
VZV	PEDA	QRL	TAH	FQSL	FC	SPHA	IMH	AKIS	SALM	DTSTSD	LVQV	NKEP...YKI	MLSDRHPIS									
EBV	.EDT	SAE	VL	A	EV	LA	CQMK	ET	TPFR	VLASR	KRSL	VTESGARSVA	PL....DCW	ILHDRHLLSA								
			172								* * 225											
HSV1	LLCY	PAARYL	MGS	MTPQ	AVL	AFVAL	I	P	P	T	N	I	V	L	G	A	L	P	E	R	.	
HSV2	LLCY	PAARYL	MGS	MTPQ	AVL	AFVAL	M	P	P	T	A	P	T	N	L	V	L	G	L	V	L	.
MHV	MVCY	PLARFM	MGC	VSLR	SVA	SLI	S	H	L	P	P	P	P	L	P	P	P	P	P	P	P	.
EHV	TVCF	PAARYL	LGD	M	S	C	A	L	M	A	M	V	A	T	L	P	R	E	P	P	P	.
VZV	TICF	PLSRYL	VGD	M	S	P	A	A	L	P	G	L	L	F	T	L	P	A	E	P	P	.
EBV	SVVF	PLMLLR	S	Q	L	S	Y	S	D	F	I	Q	V	L	A	T	P	A	D	P	G	.

TABLE I
Catalytic properties of mutant HSV 1 TKs on positions 58, 128, and 172

The left column indicates the amino acid change of each mutant. The kinetic constants (\pm S.E.) derived in this study are presented in the next three columns. The right column indicates the pH value above which full enzyme activity is attained. The values were determined by nonlinear fit of the raw data to the Michaelis-Menten equation using the Microcal Origin software. The co-substrate ATP was kept in 10–100-fold excess with regard to its K_m value (K_m of ATP, 13 μ M). The DEAE paper method (35) was applied for the kinetic measurements for wild type M128I, H58L, Y172F, and the triple mutant; for the latter, the UV-spectrometric assay was also used. + indicates that less than 3% of the activity with regard to the wt enzyme was detectable, but formation of dTMP was detectable in HPLC. – means that no activity and no formation of dTMP could be detected with neither method.

HSV 1 TK	K_m dT μ M	k_{cat} dT s^{-1}	K_m ACV m M	pH starting maximum activity
Wild type	0.20 ± 0.05	0.35 ± 0.014	0.20 ± 0.05	6.5
M128A	+	–	ND ^a	ND
M128I	0.36 ± 0.07	0.51 ± 0.039	0.51 ± 0.10	6.5
M128F	–	–	–	–
Y172F	0.51 ± 0.23	0.46 ± 0.08	+	8.5
H58L	112 ± 21	$6E-3 \pm 2E-3$	–	8.5
M128F/Y172F	–	–	–	–
H58L/M128F/Y172F	183 ± 42	$0.04 \pm 5E-3$	–	8.5

ND, not determined.

H58L/M128F/Y172F—Following the indications of the alignment studies, the His at position 58 in the completely inactive mutant M128F/Y172F was removed by subcloning to form the triple mutant H58L/M128F/Y172F. Indeed, the triple mutant turned out to regain activity and ability to phosphorylate dT with about 600-fold increased K_m . However, the phosphorylation rate was only reduced 10-fold with regard to the wild type enzyme and significantly increased compared with single mutant H58L. Attempts to phosphorylate the guanine nucleoside analog ACV that is a prototype of many other anti-herpes drugs or deoxycytidine failed even with high amounts of enzyme using the HPLC assay.

E225L—In order to explore the role of electrostatic influence in enhancing or altering substrate binding or the catalytic rate, we replaced the Glu-225 with the neutral Leu. Glu-225 forms a hydrogen bond with the 3'-OH of the deoxyribose moiety of dT that is lost by the mutation. Besides studying the consequence on affinity and velocity of thymidine kinetics, we analyzed the kinetics with AZT of wild type and mutant enzyme. The bulky, electron-rich azido group in 3'-position of AZT offers the possibility to reconnoiter the electrostatic proportions between active site and the LID region. The resulting effects are summarized in Table II. The decrease in k_{cat} and increase in K_m of the mutant toward dT compared with the wild type is more than 1 order of magnitude. However, E225L reveals the same K_m for both AZT and dT, whereas the catalytic rate of AZT conversion of E225L is increased compared with dT phosphorylation. The wild type shows an increased K_m and decreased k_{cat} for AZT

TABLE II
Kinetics of thymidine and AZT phosphorylation of mutant E225L and wild type HSV 1 TK

The kinetic constants (\pm S.E.) derived in this study are presented in the second and third columns. The values have been determined by nonlinear fit of the raw data to the Michaelis-Menten equation using the Microcal Origin software. The DEAE paper method (35) was applied for the kinetic measurements. For AZT kinetics, an additional washing step of the paper discs with ethanol 100% was necessary to remove unphosphorylated educt.

	K_m μ M	k_{cat} s^{-1}
Thymidine		
HSV 1 TK	0.2 ± 0.05	0.35 ± 0.014
E225L HSV 1 TK	12.3 ± 1.16	$0.016 \pm 3E-4$
AZT		
HSV 1 TK	5.2 ± 1.70	0.056 ± 0.013
E225L HSV 1 TK	17.0 ± 1.23	$0.032 \pm 4E-3$

phosphorylation, whereas in contrast, the mutant is capable of increasing the k_{cat} for AZT, which is the opposite of the behavior of the wild type. K_m for AZT remains within the same order of magnitude in both enzymes, indicating that the binding mode for the substrate analog seems not to be altered by the mutation.

Titration Calorimetry—We performed titration experiments with the three mutants including phenylalanine in position 128 to gain detailed insights into the reasons for the decreased binding affinities. The results are reported in Table III. The

TABLE III

Thermodynamic data for dT binding in presence of ATP of wild type HSV 1 TK and mutants including Phe at position 128

Isothermal titration microcalorimetry was performed using an OMEGA microcalorimeter. Data were collected in 50 mM Tris, pH 7.5, 4 mM EDTA, 5 mM glutathione, 1 mM DTT, and 1 mM ATP at 25 °C, corrected for ligand heats of dilution, and deconvoluted using the Microcal Origin software supplied with the instrument to yield binding constants K_a and ΔG , ΔH , and ΔS , which are the changes in free energy, enthalpy, and entropy of binding, respectively. The results of the least-squares fit assuming a single site binding model are displayed.

HSV 1 TK	ΔH	K_a	ΔG	$T\Delta S$
	<i>kcal/mol</i>	<i>M⁻¹</i>	<i>kcal/mol</i>	<i>kcal/mol</i>
Wild type	-26.35 ± 0.47	2.29E+7 ± 1.46E+7	-9.95 ± 0.40	-16.4 ± 0.85
M128F	-8.14 ± 0.20	1.04E+5 ± 1.00E+4	-6.84 ± 0.08	-1.30 ± 0.20
M128F/Y172F	-3.71 ± 0.08	3.42E+4 ± 1.85E+4	-6.14 ± 0.34	2.43 ± 0.42
H58L/M128F/Y172F	-19.82 ± 0.13	2.61E+5 ± 6.36E+3	-7.38 ± 0.01	-12.44 ± 0.14

single replacement of Met-128 by Phe (M128F) resulted in significantly increased entropy of the system, whereas the enthalpy contribution was diminished. By introduction of the second Phe, the entropy becomes even more favorable yet is responsible for establishment of binding. Because both mutants show a fairly decreased binding enthalpy, it can be suggested that the development of hydrogen bonds for thymidine is hampered, and therefore both mutants remain very weak binders. However, by complete transposition of the triad X-58/Phe-128/Phe-172, the entropy contribution adapts to the wild type value again, which enables thymidine to reappoint the correct and therefore productive hydrogen bonding. However, the binding affinity of the triple mutant remains reduced by 2 orders of magnitude. These measurements completely agree with the findings revealed by the kinetic characterization. Namely, that mutants M128F and M128F/Y172F are barely able to bind thymidine and thus not successful in phosphorylating dT, whereas the triple mutant most remarkably regains binding and phosphorylation ability. For the "inactive" mutants, this method provides even more accurate information, as they were not distinguishable from each other with the kinetic measurements.

DISCUSSION

To study binding properties and mechanisms, the possibility of purifying mutants with impaired binding affinities was an important issue. Our one-step purification protocol addressed this issue properly and was a very convenient method, allowing the purification of TK mutants not amenable to the conventional thymidine affinity resins. The subsequent thrombin cleavage led to a >90% pure thrombin-cleaved protein.

Sequence alignments have detected similarities between herpesvirus TKs and human dCK (16), and to a lesser extent cellular TmpK (17). Such similarity suggests a common ancestry of HSV TK and cellular dCK or cellular dTtmpK, although the mechanisms by which herpesviruses have acquired these genes can only be speculated upon. The superimposition of over 100 amino acids of HSV TK with the recently published crystal structures of *E. coli* and yeast dTtmpK (43, 44) reveals striking structural similarity, the latter divided into the same structural type dTtmpK as cellular dTtmpKs (45). The root mean square deviation values are markedly low, with a value of 2.5 Å, when the glycine-rich loop and the five-stranded β -sheets of yeast dTtmpK and HSV 1 TK were superimposed. Moreover, by this superimposition, the overall three-dimensional structure of HSV 1 TK, with the exception of the region between amino acid 250 and 320, was also nicely fitting to the shorter dTtmpK. A closer look at yeast and *E. coli* dTtmpK revealed, not unexpectedly, a similar binding mode for the nucleobase compared with HSV 1 TK, namely Phe-69 and the C β of Ser-98 sandwiching thymine (yeast numbering). Such meaningful structural similarity suggests, even more convincingly than sequence alignments, the evolutionary relationship among herpesviral TKs and dTtmpK. Unfortunately, to date no such material is available for dCK.

Despite the progress made in understanding detailed aspects of HSV 1 TK ligand binding, several key questions regarding the broad substrate diversity remain unresolved. In our attempt to rationalize this property, we have designed a series of HSV 1 TK mutants at the positions 58, 128, and 172 and characterized their biochemical and physicochemical properties. For the comparison of the binding behavior of the different mutants, the Michaelis constant K_m has been used as binding constant because it has been previously shown that K_m of dT ($K_m = 0.2 \mu\text{M}$) and ACV ($K_m = 200 \mu\text{M}$) correspond to the dissociation constants of dT ($K_2 = 0.139 \mu\text{M}$) and ACV ($K_5 = 162 \mu\text{M}$) (46). Furthermore, for ACV, the K_m value of 0.2 mM (Table I) corresponds with the K_i values ranging from 100 to 200 μM reported in the literature (47–49). This represents a peculiarity of HSV 1 TK by which dT is binding prior to ATP, and the rate constant of disintegration of the intermediate complex (ES) is negligible as compared to the corresponding dissociation rate constant (46).

In our study, it is noteworthy that no mutation affecting an amino acid hydrogen bonding thymidine was introduced. The combination of His-58, Tyr-172, and Met-128 in TK is hitherto only found in four viral strains, namely HSV 1, HSV 2, MHV, and BHV, causing an extensive broad substrate acceptance toward both, the sugar and base moiety of the nucleoside. Instead, in TKs that are more limited in phosphorylation with respect to the base and/or sugar moiety (50–52), the combination X-58/Phe-128/Phe-172 is found, where X can be Tyr, Phe, Ile, Met, or Pro, which are all hydrophobic. Our results emphasize the extreme sensitivity of substrate affinity on mutational changes at positions 58, 128, and 172 of HSV 1 TK.

At position 128, we have shown the role of sulfur to be purely hydrophobic. The M128I mutant constitutes a bio-isosteric modification of the wild type exhibiting almost identical affinity for thymidine and substrate analog drug ACV. This is in full agreement with previous theoretical investigations (42). We conclude that a modulation of residue size in the hydrophobic pocket at position 128 has a direct impact on binding affinity. As expected, the mutant M128A loses biological activity, which is an indication that the small alanine side chain is not sufficient to stabilize the thymine within the active site. The analysis of the structure suggests that the retained activity minimum is probably due to a partial compensation of the missing methyl group (C ϵ) of Met-128 by C δ of Ile-97 through dynamic rearrangements. Instead, the loss in biological activity of the M128F mutant is due to unproductive orientation of weakly bound thymidine, as our ITC measurements clearly indicate. The nature of the sandwich-like complex is modified by the introduction of the bulky Phe-128 into the available space provided by surrounding hydrophobic amino acids (namely Trp-88, Thr-96 (C γ), Ile-97, and Ile-100). This finding is further supported by the fact that the combination of Phe-128/Tyr-172 (HSV 1 TK numbering) sandwiching thymidine has not been found so far in any TK sequence. Additionally, the mutant with

the triad Leu-58/Phe-128/Tyr-172, another combination that does not exist in nature, shows only barely detectable dT phosphorylation.² The alteration of the flexibility of the system represented by the entropy difference between mutant and wild type may explain experimental findings showing that the mutant M128F is not able to phosphorylate thymidine. Further evidence is added by ITC measurements of this mutant in absence of ATP. The resulting binding enthalpies are the same as when titrated in the presence of ATP.³ In contrary, a substantial difference in binding affinities can be measured with the wild type enzyme under the same experimental conditions, suggesting an extended induced fit.⁴ These results imply an altered or impaired binding site for ATP in the mutant.

Similarly, the double mutant M128F/Y172F is not able to enforce catalytic turnover. The adaptation of a second Phe in the mutant M128F/Y172F even changed the sign of the entropy term, giving a hint of a favorably preformed binding pocket and of a reduction of the induced fit movement. However, the establishment of hydrogen bonds for the substrate seems to be severely impaired by this arrangement, with a more than 10-fold reduction in binding enthalpy. It can be learned from the sequence alignments that the Phe-Phe combination indeed exists, but not with a mutual His in the P loop region. In the mutants discussed above, the possibility for a reorganization upon thymidine binding is greatly impaired indicated by the already advantageous entropy of binding. Rather, removal of His is prerequisite to productive binding. The mode of binding seems to be enthalpy forced for wild type and triple mutant TK and entropy driven with M128F/Y172F.

Most striking, an additional mutation, H58L, introducing a hydrophobic leucine at the histidine position, recovers catalytic activity in the M128F/Y172F mutant. Interestingly, the exchange of His-58/Met-128/Tyr-172 to Leu-58/Phe-128/Phe-172 results in a mutant enzyme the specificity of which is mainly based on a general loss in affinity. We observed catalytic activity only toward the natural substrate, indicating a developing resistance toward purine nucleoside analogs. The rationale for the severely reduced affinity must lie in a different orientation of the base, as all the amino acids that form hydrogen bonds with dT or guanine (20) are still present. This is corroborated by our ITC measurements, revealing a ΔS similar to wild type, which indicates a restored flexibility of the enzyme. From the results, we believe the His-58/Met-128/Tyr-172 triad to be responsible for a better hydrophobic fit to natural substrates, allowing the occurrence of the successive movement for completing the catalytic cycle. As we have shown, residue 58 plays a central role in the formation of a hydrophobic pocket in a catalytically active mutant enzyme. However, the understanding of the functional role of His-58 in the binding process is not fully settled yet.

Nonetheless, on the basis of our study, we may postulate some functional roles. As can be seen in Fig. 1, the exchange of histidine 58 will presumably affect the orientation of the ribose part of the substrate. A structural variation at position 58 could indeed allow a reorientation of the ribose part, being responsible for the recovered catalytic activity in the triple mutant. His-58, positioned between Glu-225 and Glu-83, may also serve as transmitter of electron density and therefore play a central role in catalysis (together with Glu-225 and Glu-83) and electrostatics (hydrogen bond with Tyr-172) within the active site. However, the structural data and *ab initio* calculation that are so far available do not yet provide sufficient information on the role of this residue.

The mutant E225L, belonging to the LID domain, gives further support for the involvement of movement and electrostatic interaction. In the structure, Glu-225 is, together with Glu-83, the only negatively charged amino acid within a cluster of positively charged residues. Glu-225 forms a hydrogen bond with the 3'-OH of the deoxyribose moiety, which is broken by the mutation. However, the hydrogen bond of Tyr-101 to the 3'-OH is preserved (Fig. 1). The loss in affinity for dT might be explained by the missing hydrogen bond, but not the decrease in velocity. The catalytic rate is severely reduced, although all amino acids (other than Glu-225) that are involved in nucleobase binding and all the amino acids (Glu-83 and Arg-163) that are apparently involved in catalysis are disposable. Strikingly, the k_{cat} of AZT phosphorylation is faster than the k_{cat} for dT, whereas for the wild type, the opposite situation has been noticed. In TKs, the γ -phosphate of ATP and 5'-OH of deoxyribose need to be activated for the catalytic reaction. This is achieved by clusters of positive charges from the LID domain (Arg and Lys) and the Mg^{2+} , making the phosphorus atom amenable for a nucleophilic attack of the polarized 5'-O, which is positioned between Glu-225 and Glu-83 (19) and needs to be negatively charged. During AZT phosphorylation, Glu-225 of wild type HSV 1 TK is displaced by the bulky 3'-azido group of AZT (53), which leads to a reduction of polarization of the 5'-O, with a consequent decrease in velocity. In the E225L mutant, the decline in velocity lies within the same order of magnitude. This finding suggests that either displacement or removal of the negative charge (Glu-225) results in an equal effect. By searching for similar features in dTnpK, we found Asp-14 in yeast and Glu-12 in *E. coli* dTnpK that might take over the function of both Glu-225 and Glu-83 in polarizing 3'-OH of the deoxyribose and of one oxygen of the α -phosphate of dTMP.

It is noteworthy that our mutagenesis study on the triad involved residues without direct hydrogen bond contact with the substrate, underscoring the capability of hydrophobic contacts and electrostatics. The residues maintaining direct hydrogen bonds, rather, guide resistance patterns (29). Our results emphasize the extreme sensitivity of substrate affinity and diversity on mutational changes at the HSV 1 TK positions 58, 128, and 172. This finding is in complete agreement with our sequence alignment study, indicating the residue triad His-58, Tyr-172, and Met-128 to be a common motif in thymidine kinases with broad substrate diversity, whereas variations at these positions, which correspond to the X-58/Phe-128/Phe-172 HSV 1 TK mutations, are a common feature for enzymes with restricted substrate acceptance. Our findings indicate that the existence of a structurally flexible sandwich complex and the maintenance of balanced electrostatics are crucial for substrate diversity in HSV 1 TK and a plausible evolutionary pattern. Therefore, we add a new piece of information for the design of new antiviral drugs and modified TKs for gene therapy of cancer and AIDS.

Acknowledgments—We thank Dr. I. Jelesarov for constructive discussion and technical assistance with the ITC measurements, U. Kessler for aid with the HPLC, F. Seegy for assistance with the figures, and P. Pospisil for support in the structural comparison of dTnpK.

REFERENCES

- Chen, M. S., and Prusoff, W. H. (1978) *J. Biol. Chem.* **253**, 1325–1327
- Chen, M. S., Summers, W. P., Walker, J., Summers, W. C., and Prusoff, W. H. (1979) *J. Virology* **30**, 942–945
- Koonin, E. V., and Senkevich, T. G. (1992) *Virus Genes* **6**, 187–196
- Cheng, Y. C., Huang, E. S., Lin, J. C., Mar, E. C., Pagano, J. S., Dutschman, G. E., and Grill, S. P. (1983) *Proc. Natl. Acad. Sci. U. S. A.* **80**, 2767–2770
- Elion, G. B., Furman, P. A., Fyfe, J. A., de Miranda, P., Beauchamp, L., and Schaeffer, H. J. (1977) *Proc. Natl. Acad. Sci. U. S. A.* **74**, 5716–5720
- Keller, P. M., Fyfe, J. A., Beauchamp, L., Lubbers, C. M., Furman, P. A., Schaeffer, H. J., and Elion, G. B. (1981) *Biochem. Pharmacol.* **30**, 3071–3077

³ R. Perozzo, unpublished observation.

⁴ R. Perozzo, manuscript in preparation.

7. Culver, K. W., Van Gilder, J., Link, C. J., Carlstrom, T., Buroker, T., Yuh, W., Koch, K., Schabold, K., Doornbas, S., and Wetjen, B. (1994) *Hum. Gene Ther.* **5**, 343–379
8. Tong, X. W., Agoulnik, I., Blankenburg, K., Contant, C. F., Hasenburg, A., Runnebaum, L. B., Stickeler, E., Kaplan, A. L., Woo, S. L., and Kieback, D. G. (1997) *Anticancer Res.* **17**, 811–813
9. Caruso, M., and Bank, A. (1997) *Virus Res.* **52**, 133–143
10. Bonini, C., Ferrari, G., Verzeletti, S., Servida, P., Zappone, E., Ruggieri, L., Ponzoni, M., Rossini, S., Mavilio, F., Traversari, C., and Bordignon, C. (1997) *Science* **276**, 1719–1724
11. Jacobson, J. G., Chen, S. H., Cook, W. J., Kramer, M. F., and Coen, D. M. (1998) *Virology* **242**, 161–169
12. Efstathiou, S., Kemp, S., Darby, G., and Minson, A. C. (1989) *J. Gen. Virol.* **70**, 869–879
13. Coen, D. M., Kosz-Vnenchak, M., Jacobson, J. G., Leib, D. A., Bogard, C. L., Schaffer, P. A., Tyler, K. L., and Knipe, D. M. (1989) *Proc. Natl. Acad. Sci. U. S. A.* **86**, 4736–4740
14. Chen, S. H., Cook, W. J., Grove, K. L., and Coen, D. M. (1998) *J. Virol.* **72**, 6710–6715
15. Bradshaw, H. D., Jr., and Deininger, P. L. (1984) *Mol. Cell. Biol.* **4**, 2316–2320
16. Harrison, P. T., Thompson, R., and Davison, A. J. (1991) *J. Gen. Virol.* **72**, 2583–2586
17. Robertson, G. R., and Whalley, J. M. (1988) *Nucleic Acids Res.* **16**, 11303–11317
18. Wild, K., Bohner, T., Aubry, A., Folkers, G., and Schulz, G. E. (1995) *FEBS Lett.* **368**, 289–292
19. Wild, K., Bohner, T., Folkers, G., and Schulz, G. E. (1997) *Protein Sci.* **6**, 2097–2106
20. Brown, D. G., Visse, R., Sandhu, G., Davies, A., Rizkallah, P. J., Melitz, C., Summers, W. C., and Sanderson, M. R. (1995) *Nat. Struct. Biol.* **2**, 876–881
21. Muller, C. W., Schlauderer, G. J., Reinstein, J., and Schulz, G. E. (1996) *Structure* **4**, 147–156
22. Liu, Q. Y., and Summers, W. C. (1988) *Virology* **163**, 638–642
23. Munir, K. M., French, D. C., Dube, D. K., and Loeb, L. A. (1992) *J. Biol. Chem.* **267**, 6584–6589
24. Munir, K. M., French, D. C., Dube, D. K., and Loeb, L. A. (1994) *Protein Eng.* **7**, 83–89
25. Balasubramaniam, N. K., Veerisetty, V., and Gentry, G. A. (1990) *J. Gen. Virol.* **71**, 2979–2987
26. Englund, J. A., Zimmerman, M. E., Swierkosz, E. M., Goodman, J. L., Scholl, D. R., and Balfour, H. H., Jr. (1990) *Ann. Intern. Med.* **112**, 416–422
27. Darby, G., Field, H. J., and Salisbury, S. A. (1981) *Nature* **289**, 81–83
28. Gaudreau, A., Hill, E., Balfour, H. H., Jr., Erice, A., and Boivin, G. (1998) *J. Infect. Dis.* **178**, 297–303
29. Kussmann-Gerber, S., Kuonen, O., Folkers, G., Pilger, B. D., and Scapozza, L. (1998) *Eur. J. Biochem.* **255**, 472–481
30. Michael, M., Gerber, S., Fetzter, J., and Folkers, G. (1997) *Pharm. Acta Helv.* **72**, 139–143
31. Steinberg, R. A., and Gorman, K. B. (1994) *Anal. Biochem.* **219**, 155–157
32. Barettino, D., Feigenbutz, M., Valcarcel, R., and Stunnenberg, H. G. (1994) *Nucleic Acids Res.* **22**, 541–542
33. Innis, M. A., Gelfand, D. H., Sninsky, J. J., and White, T. J. (eds) (1990) *PCR Protocols: A Guide to Methods and Application*, pp. 177–183, Academic Press Inc., San Diego
34. Fetzter, J., Michael, M., Bohner, T., Hofbauer, R., and Folkers, G. (1994) *Protein Expression Purif.* **5**, 432–441
35. Gerber, S., and Folkers, G. (1996) *Biochem. Biophys. Res. Commun.* **225**, 263–267
36. Furlong, N. B. (1963) *Anal. Biochem.* **5**, 515–522
37. Masson, S., Desmoulin, F., Sciaky, M., and Cozzone, P. J. (1993) *Biochemistry* **32**, 1025–1031
38. Wiseman, T., Williston, S., Brandts, J. F., and Lin, L. N. (1989) *Anal. Biochem.* **179**, 131–137
39. Corpet, F. (1988) *Nucleic Acids Res.* **16**, 10881–10890
40. Folkers, G., and Trumpp, S. (1987) *Med. Sci. Res.* **15**, 1495–1496
41. Halpern, M. E., and Smiley, J. R. (1984) *J. Virol.* **50**, 733–738
42. Alber, F., Kuonen, O., Scapozza, L., Folkers, G., and Carloni, P. (1998) *Proteins* **31**, 453–459
43. Lavie, A., Vetter, I. R., Konrad, M., Goody, R. S., Reinstein, J., and Schlichting, I. (1997) *Nat. Struct. Biol.* **4**, 601–604
44. Lavie, A., Ostermann, N., Brundiars, R., Goody, R. S., Reinstein, J., Konrad, M., and Schlichting, I. (1998) *Proc. Natl. Acad. Sci. U. S. A.* **95**, 14045–14050
45. Lavie, A., Konrad, M., Brundiars, R., Goody, R. S., Schlichting, I., and Reinstein, J. (1998) *Biochemistry* **37**, 3677–3686
46. Kussmann-Gerber, S., Wurth, C., Scapozza, L., Pilger, B. D., Pliska, V., and Folkers, G. (1999) *Nucleosides Nucleotides* **18**, 311–330
47. Fyfe, J. A., McKee, S. A., and Keller, P. M. (1983) *Mol. Pharmacol.* **24**, 316–323
48. Larder, B. A., Cheng, Y. C., and Darby, G. (1983) *J. Gen. Virol.* **64**, 523–532
49. Larder, B. A., Derse, D., Cheng, Y. C., and Darby, G. (1983) *J. Biol. Chem.* **258**, 2027–2033
50. Abele, G., Cox, S., Bergman, S., Lindborg, B., Vissgarden, A., Karlström, A., Harmenberg, J., and Wahren, B. (1991) *Antiviral Chem. Chemother.* **2**, 163–169
51. Roberts, G. B., Fyfe, J. A., McKee, S. A., Rahim, S. G., Daluge, S. M., Almond, M. R., Rideout, J. L., Koszalka, G. W., and Krenitsky, T. A. (1993) *Biochem. Pharmacol.* **46**, 2209–2218
52. Gustafson, E. A., Chillemi, A. C., Sage, D. R., and Fingerroth, J. D. (1998) *Antimicrob. Agents Chemother.* **42**, 2923–2931
53. Christians, F., Scapozza, L., Cramer, A., Folkers, G., and Stemmer, P. W. (1999) *Nat. Biotechnol.* **17**, 259–264